Thin Solid Films, Volume 518, Issue 14, 3 May 2010, Pages 3763-3766

Study of compositional change in the interfacial regions between lead strontium titanate (PST)/SiO_2 and lead zirconate titanate (PZT)/SiO_2 by Auger Emission Spectroscopy

Arne Lüker[a, b], Qi Zhang[a], and Paul B. Kirby[a]

a) *Materials Department, Cranfield University, Bedford MK43 0AL, UK*

b) Contact details: Wachtelweg 11, 32609 Hüllhorst/Holsen, Germany

email: arnelueker@aim.com

Telephone: +49 (0)5744 5074749

or Skype

Abstract: Auger spectroscopy was used to study the compositional change in the interfacial region between ferroelectric thin films, namely lead strontium titanate (PST) and lead zirconate titanate (PZT), and commercial available Si substrates with a 200 nm thick thermal oxide layer. Both PST and PZT thin films were prepared via a sol-gel spin coating method. The thin films from both materials were annealed under the same conditions (temperature and time). It was found that strontium stops the lead diffusion into SiO_2 by forming $SrTiO_3$ and/or SrO, maintaining a well defined SiO_2 region, while $PbSiO_3$ is formed in the PZT/SiO_2 system. These results are important for a general understanding of interdiffusions in material interfaces in particular for the realization of future high-dielectric-constant (high-k) oxide layers and for the next generation of advanced electronic devices.

Keywords: PST, lead strontium titanate, PZT, lead zirconate titanate, sol-gel, SiO_2, silicon dioxide, interdiffusion, diffusion, barrier layer, AES, Auger emission spectroscopy, lead silicate, depth profile

1. Introduction:

Surface diffusion not only plays an important role in atomic processes on the surface of solids but also is one major issue one meets when following the new international technology roadmap for semiconductors (ITRS) [1]. It is stated that the thickness of SiO_2 gate oxides has to be less than 2 nm in the near-term technology requirements. Despite the problem that the gate leakage current will approach the ITRS-defined limit of 1 A/cm^2 with an applied gate voltage of 3 V when the gate oxide thickness is less than 2 nm [2], this aim also demands new requirements on diffusion barriers. Atomic diffusion between material interfaces is one of the main reasons for failures within electronic chip devices like memories and therefore an important subject when talking about reliability of MEMS.

When it comes to the integration of ferroelectrics the problem becomes worse because the most used ferroelectric perovskite thin film today is PZT and Pb is notorious to diffuse deep into the silicon substrate [3, 4], even through a TiO_2-diffusion barrier and Ti/Pt bottom electrode. $SrTiO_3$, a centrosymmetric paraelectric material with a perovskite structure, was used as a buffer layer and template for the integration of PZT [5 - 7] or as a dielectric layer itself on top of Si to replace SiO_2 as a common gate oxide [8 – 12]. It was shown that SrO grows first epitaxially even on H-terminated Si surfaces with a sharp interface and thus provides an ionic template for the subsequent growths of perovskite $SrTiO_3$ [8, 10, 12]. We showed earlier that a functional PST layer (thickness > 300 nm) grows directly on top of SiO_2 [13] and that a very thin PST film (thickness < 50 nm) can serve as a barrier layer and template for the growths of PZT on top of SiO_2 [14]. However, a direct comparison between the interfacial regions of PST/SiO_2 and PZT/SiO_2 is still outstanding. The purpose of this

paper is to study these interfaces using Auger Emission Spectroscopy and to develop a more profound understanding of Pb-diffusion and the role of Sr as a barrier layer.

2. Experimental Procedure

The preparation of the starting solutions of $Pb(Zr_{30}Ti_{70})O_3$ and $(Pb_{40}Sr_{60})TiO_3$ was described earlier [13 – 16].

Both solutions were spin coated at 3000 rpm for 30 s on Si substrates with a 200 nm thick thermal SiO_2 layer. The films were dried and pyrolysed on a hotplate at 350 °C for 10 min and subsequently annealed at 650 °C for 15 min on a second hotplate. The resulting thicknesses of the films were ~ 50 nm. The annealing temperature of 650 °C is the crystallisation temperature of PST and is higher than for PZT, which has a crystallisation temperature < 600 ºC. According to Fick's and Arrhenius laws, diffusion is time and temperature dependent, therefore these variables should be held constant to compare the interdiffusion character in both material systems. The chosen temperature and time in this study were those for the crystallisation of PST, viz. 650 °C for 15 min.

A VG ESCAlab Mk 2 Auger Emission Spectrometer (AES) was used to analyse the compositional change in the interfacial region. AES has the ability to provide excellent lateral resolution, allowing reliable analysis of very small areas (less than 1 micron). It also offers satisfactory sensitivity, detecting elements that are less than 1% of the atomic composition of the sample. The output of AES is referred to as an Auger spectrum. This spectrum would show peaks at Auger electron energy levels corresponding to the atoms from which the auger electrons were released - sometimes called binding energy. In order to detect the composition of a sample along the sample depth, a crater must first be milled on the sample at the correct depth by ion-sputtering. After each sputtering step the Auger spectrum is measured, followed by another sputtering step and so on.

3. The Interface between PST and SiO_2/Si

Fig. 1 shows the Auger spectra that reflect compositional changes in the interfacial region between PST and SiO_2/Si. After each measurement, the sample was etched for 100 s using the ion-sputtering unit with an ion beam output of 2 kV and 0.75 µA (1.5 mW).

The dark blue trace, which is best seen at the top of the titanium peak at 462 eV, indicates the first measurement without an etching step. At this point only the lead peaks at 137 and 144 eV, the strontium peaks at 135 and 272 eV and the oxygen peak at 535 eV are traceable furthermore. The intensities of these peaks decrease with increasing etching time. After the fifth etching step (the brownish red trace) the Si-O peaks at 105 eV and 536 eV begin to appear. That marks the beginning of the interfacial layer. The positions of these two peaks shift to higher energies and the intensities increase with increasing etching time while the titanium, lead, strontium and oxygen peaks of the PST layer decrease. Finally, after the 14^{th} etching step (the orange trace) the PST peaks vanish and the spectra only show the Si-O peaks, indicating the end of the interfacial layer.

The SiO_2 layer is comparably thick. Nearly forty etching steps are needed to reach the main Si substrate as depicted in Fig. 2. After that only the main Si-Si bond at ~100 eV is traceable.

Fig. 3 shows the corresponding depth profile. It should be noted that the unit of the abscissa is etch cycle number. Different elements and/or compounds, normally have different etch rates; therefore it is impossible to make a clear statement of the real thickness without knowing the specific etch rates. However, we know that the SiO_2 layer is 200 nm and the PST layer ~50 nm thick, leading to an etch rate of approximately 0.029 nm/(mW·s) and 0.033 nm/(mW·s) for SiO_2 and PST respectively.

The diffusion area of the PST/SiO_2 interface is relatively small. After ten etching steps the diffusion of titanium and lead stops. Only strontium diffuses further on until it is not traceable anymore after the 14^{th} etching step (inset in Fig. 3). The silicon diffuses stronger into the PST

layer due to the large Si-source. The broad SiO_2 area is the dominant feature in this profile and the SiO_2/Si interface is clearly distinguishable.

4. The Interface between PZT and SiO_2/Si

As a comparison a single layer of PZT was deposited directly onto SiO_2/Si. It is well known that Pb in PZT strongly diffuses into the substrate [3], therefore 10% Pb excess is normally given to the solution to compensate the Pb loss during the heat treatment of the thin film. The depth profile of this sample is shown in Fig. 4.

The etch rates in this system are considerably lower compared to the PST sample. The etching parameters were adjusted to 100 s, 2 kV and 0.9 µA (1.8 mW) for each etch step. Although that means a higher ion beam output more etch cycles were needed to reach a comparable depth. Assuming the same layer thicknesses as PST this leads to an etch rate of 0.009 nm/(mW·s) for PZT and 0.012 nm/(mW·s) for the SiO_2 interdiffusion layer. The lower etch rate of the latter layer was explained by a formation of some lead silicate ($PbSiO_3$), which is harder to etch than SiO_2 using the ion sputtering unit [17].

Fig. 5 shows the details of the Auger analysis for Pb, O and Si traces. The first two traces after etch cycles 15 and 32 (top blue and magenta in the Pb and O spectra) show that Pb and O are present in a similar way like in Fig.1, viz a Pb double peak at 140 and 146 eV and an O_{PZT} peak at 536 eV. The Si is not really traceable in this region. After etch cycle 54 (thick black curve) a second O peak begins to appear at 539 eV and the Si shows two weak peaks at 102 and 107 eV. At the same time the Pb double peak moves slightly to lower energies and begins to “wobble” around with increasing depth until it vanishes after the 94^{th} etch cycle (thick blue curve). After the Pb is not traceable anymore O shows only one peak at higher energy and the Si only one at lower energy. The oxygen peak is decreasing and the Si is increasing while shifting again to higher energies with further etch cycles.

These results indicate that the region between the 54th and the 94th etch cycle can be regarded as the main diffusion area of these three elements. The appearance of the second O peak and the Si double peak, together with the shift of the Pb peak to lower energies indicates further on a bonding mechanism between Pb, O and Si. The rocking motion of the Pb double peak system and the disappearance of the Si peak at 107 eV may be explained by a variable stoichiometric composition of these three. However, the formation of some lead silicate $xPbO(1-x)SiO_2$ in this region is the most likely process to explain this behavior.

5. Conclusions

Fig. 4 and 3 show that the Pb diffusion into Si from the PZT thin film is significantly higher than from the PST thin film. Sr diffuses slightly more into the SiO_2 layer than Ti in Fig. 3, followed by Pb, which diffusion stops almost immediately, whereas in Fig. 4 Pb, Zr and Ti are diffusing to the same extent. The shift of the Sr peaks in Fig. 3 after etch step 11, 12, and 13 to higher energies indicates that the Sr changes its bonding partner towards SiO_2. This demonstrates that Sr grows first on top of the SiO_2 layer and makes it chemically inert to further oxidisation or possible reactions with other elements, thus preventing interdiffusion in both ways.

While Si is a covalently bonded material, PST is an ionic crystal that is unable to form covalent bonds. An electronically saturated Si-PST stack must thus exhibit an interfacial layer which provides a covalent bonding environment towards the silicon substrate and in addition an ionic template compatible with that of PST or $SrTiO_3$. SrO covalently saturates all Si dangling bonds by forming $SrSiO_3$ and/or Sr_2SiO_4. This provides the necessary ionic template towards the perovskite SrO-terminated $SrTiO_3$, on which PST can grow further on.

Remarkable is furthermore the missing of a clear distinct SiO_2 region in Fig. 4. It is assumed that the formation of some lead silicate in this region may be a possible explanation. This would also explain the lower etching rate in the PZT system.

All these results show that the $SrTiO_3$ is an effective diffusion barrier on top of SiO_2/Si. It inhibits the interdiffusion of all components of PST into the SiO_2/Si and vice versa. These offers the possibility to realise a thin interfacial layer for future integrations of ferroelectrics in all kind of devices like non-destructive read out ferroelectric RAMs [5, 9, 11, 12] or simply as a buffer layer for the realization of ferroelectrics onto Si without the common Ti/Pt bottom electrode [5 – 7,13].

6. Acknowledgements

The authors would like to thank Mr. Andrew Stallard and Mr. Matthew Taunt for their never ending effort to keep our labs running and Dr. Matthew Kershaw for his help with the AES Analysis and fruitful discussions. This research was supported by EPSRC (EP/C520297/1).

7. References

1. International Technology Roadmap for Semiconductors, Semiconductor Industry Association, Austin, Texas, 2007

2. A.I. Klingon, J. Maria, S.K. Streiffer, Nature 406 (2000) 1032

3. A.E. Dolbak, R.A. Zhachuk, and B.Z. Olshanetsky; CEJP 2(2) 2004 254-265

4. Y. Zhu, P. Yan, T. Yi, L. Cao, and L. Li; Surf. Interface Anal. 27, 972-980 (1999)

5. D.S. Shin, S.T. Park, H.S. Choi, I.H. Choi, and J.Y. Lee; Thin Solid Films 354 (1999) 251-255

6. Y. Wang, C. Ganpule, B.T. Liu, H. Li, K. Mori, B. Hill, M. Wuttig, R. Ramesh, J. Finder, Z. Yu, R. Droopard, and K. Eisenbeiser; Applied Physics Letters 80 (1), 2002

7. B.T. Liu, K. Maki, Y. So, V. Nagarajan, R. Ramesh, J. Lettieri, J.H. Haeni, D.G. Schlom, W. Tian, X.Q. Pan, F.J. Walker, and R.A. Mc Kee; Applied Physics Letters 80 (25), 2002

8. C.J. Först, C.R. Ashman, K. Schwarz, and P.E. Blöchl; Nature 427 (2004)

9. C.C. Lin, L.W. Lai, C.Y. Lin, and T.Y. Tseng; Thin Solid Films xx (2006) xxx-xxx

10. Y. Machida, H. Asaoka, H. Yamamoto, and S. Shamoto; Surface Science 600 (2006) 724-128

11. X. Hu, H. Li, Y. Liang, Y. Wie, Z. Yu, D. Marshall, J. Edwards, R. Droopad, X. Zhang, A.A. Demkov, K. Moore, and J. Kulik; Applied Physics Letters 82 (2), 2003

12. Md.N.K. Bhuiyan, H. Kimura, T. Tambo, and C. Tatsuyama; Applied Surface Science 249 (2005) 419-424

13. Y-H-. Chun, C. Fragkiadakis, P. Bao, A. Lüker, R.V. Wright, J-S. Hong, P.B. Kirby, Q. Zhang, T.J. Jackson, M.J. Lancester, "Tunable Bandstop Resonators and Filter on Si-Substrate with PST Thin Film by Sol-Gel Deposition", 38th European Microwave Conference, EuMC2008

14. D. Bhattacharyya, A. Lüker, Q. Zhang and P.B. Kirby, submitted *to Thin Solid Films,* "Structural evaluation of sol-gel derived lead strontium titanate diffusion barrier for integration in PZT transducer design", *2009*

15. Q. Zhang, R.W. Whatmore, Journal of Physics D: Applied Physics, 34 (2001) 2296, " Sol-gel PZT and Mn-doped PZT thin films for pyroelectric applications".

16. Yi G, Wu Z and Sayer M, "Preparation of $Pb(Zr,Ti)O_3$ thin films by sol gel processing: Electrical, optical, and electro-optic properties", J. Appl. Phys., Vol. 64(5), p.2717-24, September, 1988

17. Communication with Dr. Matthew Kershaw.

Figure Caption:

Fig. 1: Auger spectra of one layer PST and its interface to the SiO_2. Between each measurement the sample was etched for 100 sec using the ion-sputtering unit with an ion current of 2kV and 0.75µA

Fig. 2: Auger spectra of the SiO2 layer (a) and its interface to the Si main substrate (b).

Fig. 3: Depth profile of one layer PST on SiO_2/Si – a close up towards the first 15 etch cycles is presented in the inset. The interface regions are clearly visible

Fig. 4: Depth profile of one layer PZT on SiO_2/Si. The interface regions are blurred.

Fig. 5: Details of the Auger analysis for Pb, Oxygen and Si in the interfacial region of PZT on SiO2/Si. The main interdiffusion area is between the etch cycle 54 (black, thick trace) and the etch cycle 94 (blue, thick trace)

Fig. 1

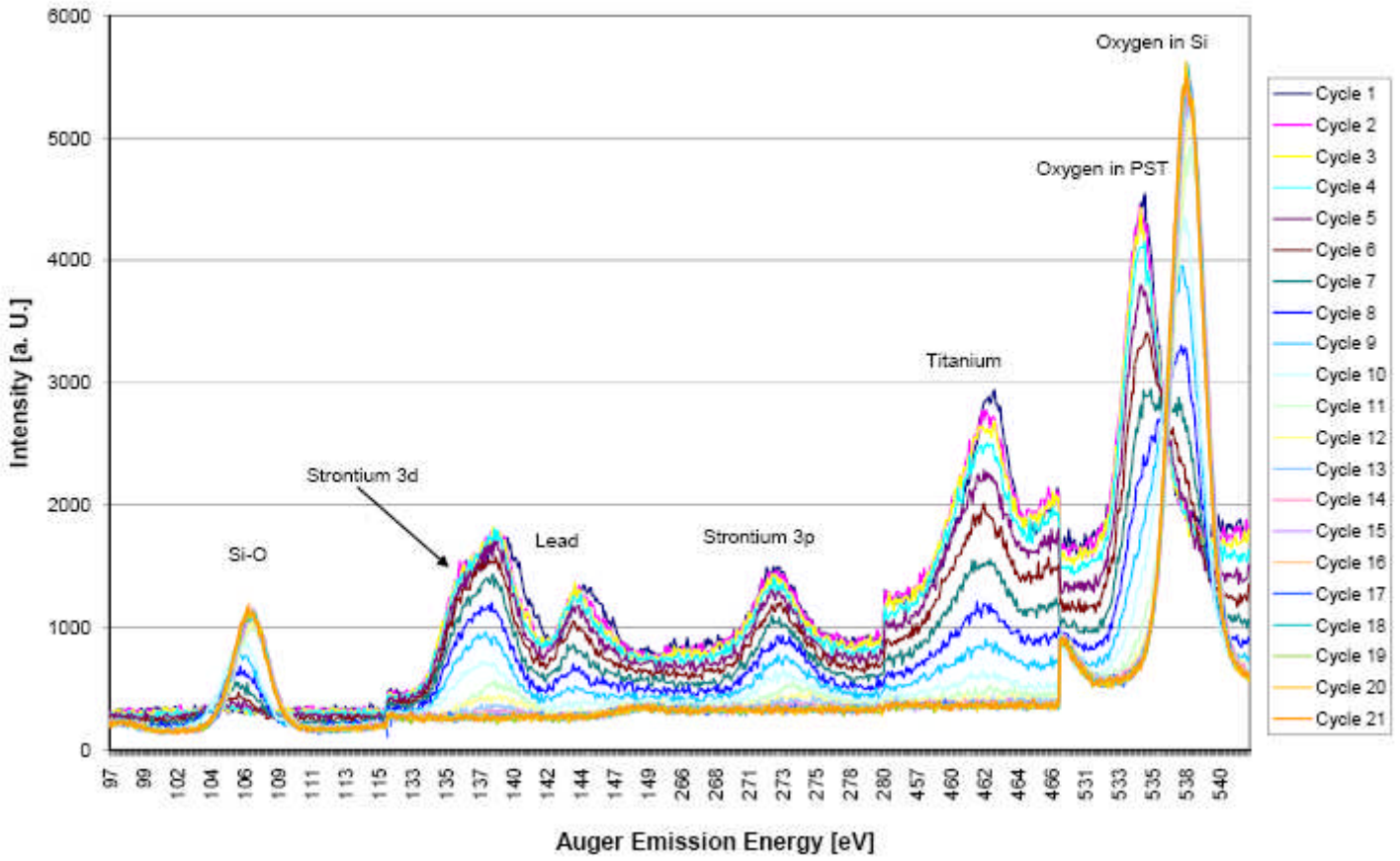

Oxygen in Si
Oxygen in PST
Titanium
Strontium 3d
Lead
Strontium 3p
Si-O
Intensity [a. U.]
Auger Emission Energy [eV]
Cycle 1
Cycle 2
Cycle 3
Cycle 4
Cycle 5
Cycle 6
Cycle 7
Cycle 8
Cycle 9
Cycle 10
Cycle 11
Cycle 12
Cycle 13
Cycle 14
Cycle 15
Cycle 16
Cycle 17
Cycle 18
Cycle 19
Cycle 20
Cycle 21

Fig. 2

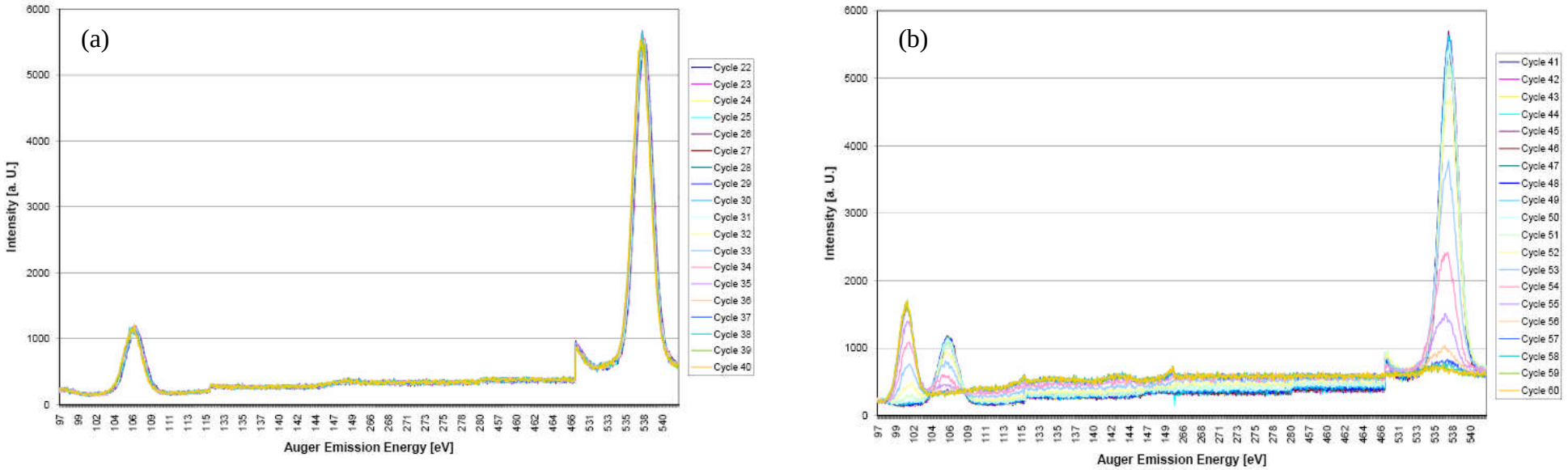

(a)
Intensity [a. U.]
Auger Emission Energy [eV]
Cycle 22
Cycle 23
Cycle 24
Cycle 25
Cycle 26
Cycle 27
Cycle 28
Cycle 29
Cycle 30
Cycle 31
Cycle 32
Cycle 33
Cycle 34
Cycle 35
Cycle 36
Cycle 37
Cycle 38
Cycle 39
Cycle 40
(b)
Intensity [a. U.]
Auger Emission Energy [eV]
Cycle 41
Cycle 42
Cycle 43
Cycle 44
Cycle 45
Cycle 46
Cycle 47
Cycle 48
Cycle 49
Cycle 50
Cycle 51
Cycle 52
Cycle 53
Cycle 54
Cycle 55
Cycle 56
Cycle 57
Cycle 58
Cycle 59
Cycle 60

Fig. 3

Fig. 3

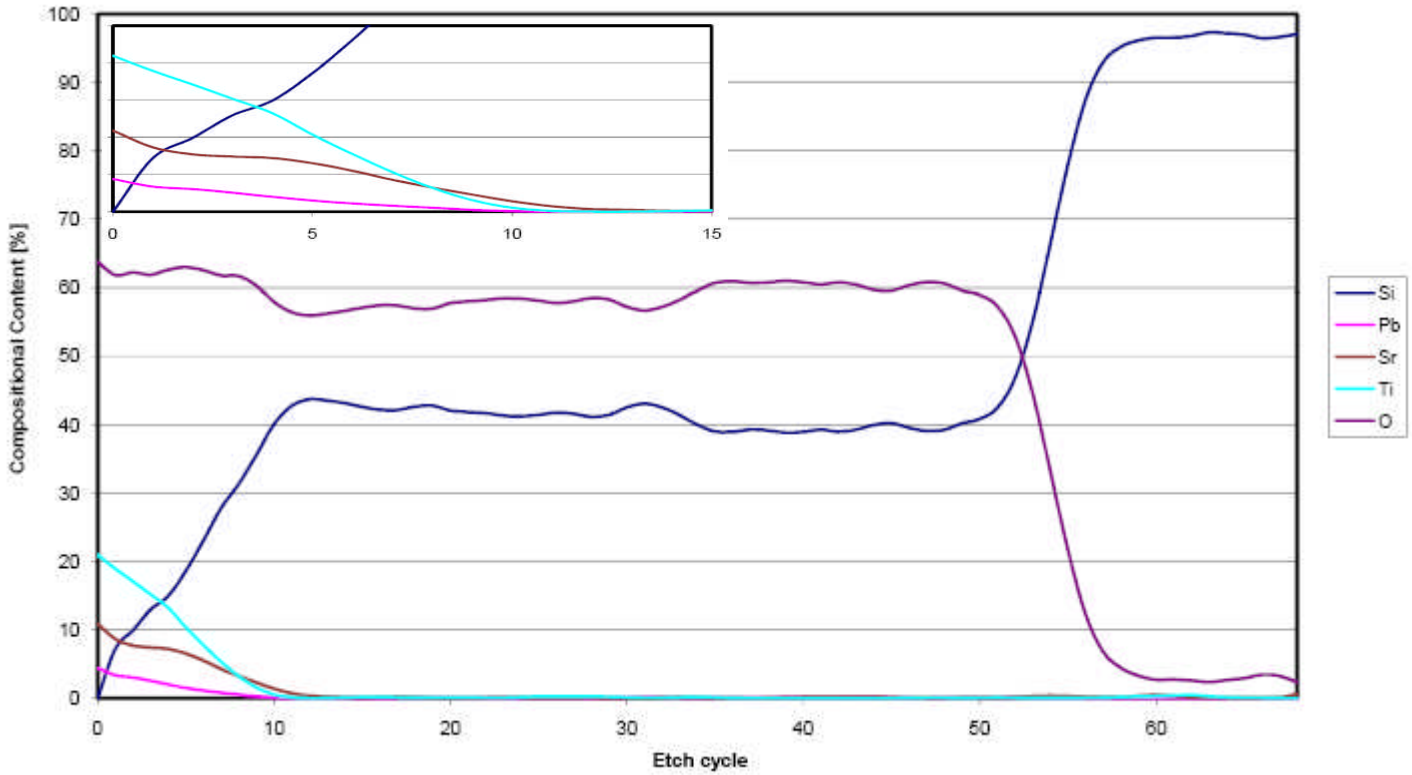


Fig. 4

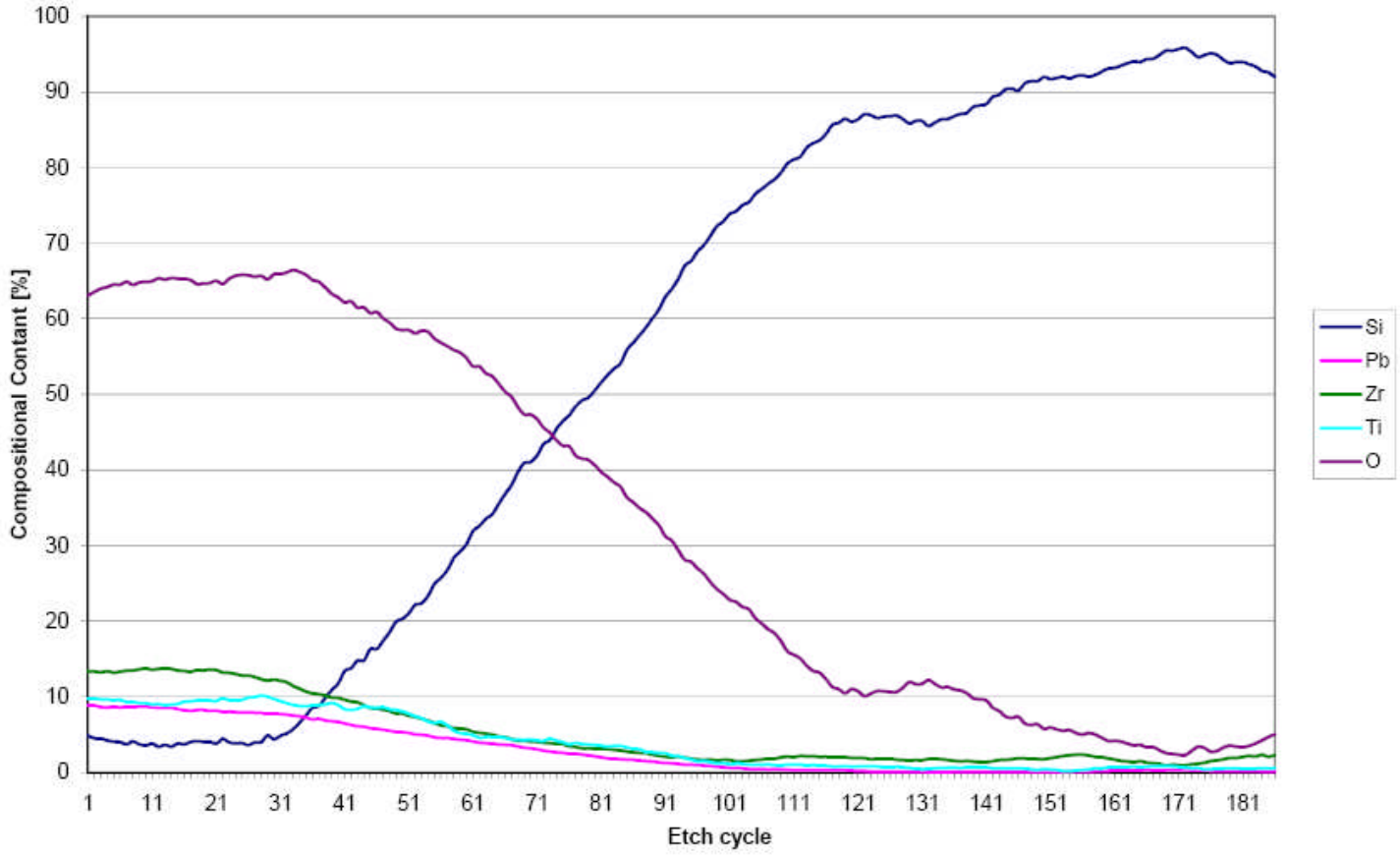
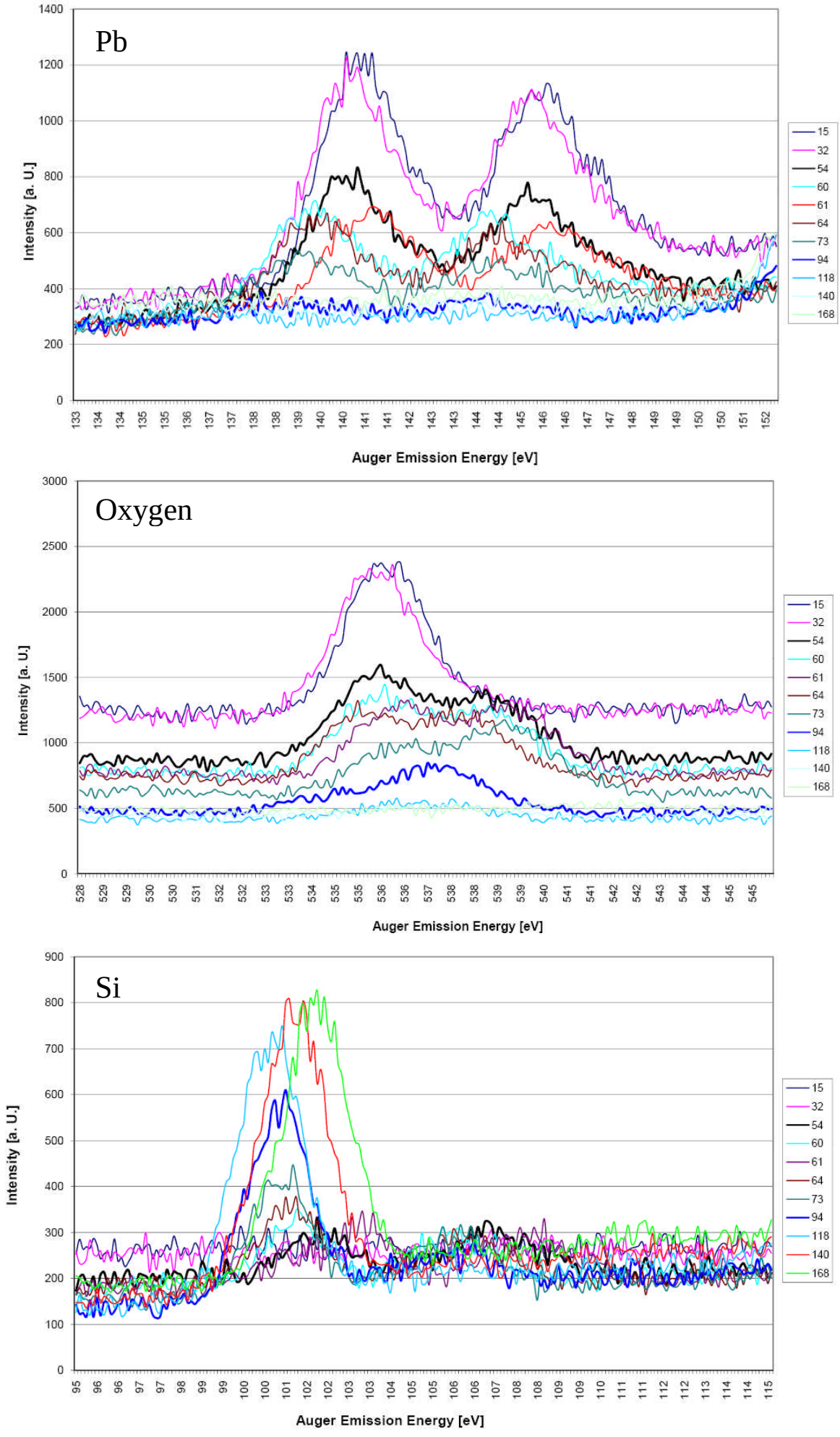

100
90
80
70
60
50
40
30
20
10
0
Compositional Contant [%]
1
11
21
31
41
51
61
71
81
91
101
111
121
131
141
151
161
171
181
Etch cycle
Si
Pb
Zr
Ti
O

Fig. 5


Pb
Intensity [a. U.]
Auger Emission Energy [eV]
15
32
54
60
61
64
73
94
118
140
168
Oxygen
Intensity [a. U.]
Auger Emission Energy [eV]
15
32
54
60
61
64
73
94
118
140
168
Si
Intensity [a. U.]
Auger Emission Energy [eV]
15
32
54
60
61
64
73
94
118
140
168



https://dspace.org/

Study of compositional change in the interfacial regions between lead strontium titanate (PST)/SiO2 and lead zirconate titanate (PZT)/SiO2 by Auger emission spectroscopy

Luker, Arne; Zhang, Qi; Kirby, Paul B.

2010-05-03T00:00:00Z
Elsevier Science B.V., Amsterdam.
http://dx.doi.org/10.1016/j.tsf.2009.11.018
Arne Luker, Qi Zhanga and Paul B. Kirby. Study of compositional change in the interfacial regions between lead strontium titanate (PST)/SiO2 and lead zirconate titanate (PZT)/SiO2 by Auger emission spectroscopy. Thin Solid Films, Volume 518, Issue 14, 3 May 2010, Pages 3763-3766

Downloaded from a DSpace repository. https://dspace.org/